Probing Spin States of Coupled Quantum dots by dc Josephson Current

Yu Zhu[1], Qing-feng Sun[2], and Tsung-han Lin[1,*]

State Key Laboratory for Mesoscopic Physics and Department of Physics, Peking University, Beijing, 100871, China[1]

Center for the Physics of Materials and Department of Physics, McGill University, Montreal, PQ, Canada H3A 2T8[2]

()

Abstract

We propose an idea for probing spin states of two coupled quantum dots (CQD), by the dc Josephson current flowing through them. This theory requires weak coupling between CQD and electrodes, but allows arbitrary inter-dot tunnel coupling, intra- and inter- dot Coulomb interactions. We find that the Coulomb blockade peaks exhibit a non-monotonous dependence on the Zeeman splitting of CQD, which can be understood in terms of the Andreev bound states. More importantly, the supercurrent in the Coulomb blockade valleys may provide the information of the spin states of CQD: for CQD with total electron number N=1,3 (odd), the supercurrent will reverse its sign if CQD becomes a magnetic molecule; for CQD with N=2 (even), the supercurrent will decrease sharply around the transition between the spin singlet and triplet ground states of CQD.

PACS numbers: 74.50.+r, 73.40.Gk, 73.20.Dx, 72.15.Nj.

Coupled quantum dots (CQD) fabricated in semiconductors, or so called "artificial molecule", is an ideal quantum system for the study of coherent transport. Each quantum dot (QD) contains discrete energy levels (quantized due to spacial confinement), which can be tuned independently by the gate voltages. The coupling between the dots is also adjustable, resulting in either "ionic molecule" for weak coupling or "covalent molecule" for strong coupling. The electron-electron interactions play an essential role in the transport properties of CQD, due to that the electrons are added to the molecule one by one, and the conductance exhibits Coulomb blockade oscillations. Such appealing system has attracted a lot of experimental and theoretical attentions, such as the observations of Coulomb blockade in double or triple quantum dots [1–4]; the measurement of microwave spectroscopy of a quantum dot molecule and the comparison with the time dependent theory [5–7]; the analysis of the additional spectra of CQD in the magnetic field by using single electron capacitance spectroscopy [8]; the investigations of electronic correlations and Kondo effect in CQD by two impurity Anderson model [9,10], and much more.

Nevertheless, the spin -dependent transport through CQD are less addressed [11,12]. For a single QD, it was proposed recently that QD in the Coulomb blockade regime may act as an efficient spin filter in the presence of magnetic field [13]. For coupled double QDs, the spin related physics is even more rich. Consider CQD filled with two excess electrons, each dot occupied by one of them because of the large on-site Coulomb repulsion. CQD in this case may have four spin configurations: $|1\uparrow 2\uparrow\rangle$, $|1\downarrow 2\downarrow\rangle$, $|1\uparrow 2\downarrow\rangle$, $|1\downarrow 2\uparrow\rangle$, as shown in the lower part of Fig.1. Due to the inter-dot tunneling processes, $|1\uparrow 2\downarrow\rangle$ and $|1\downarrow 2\uparrow\rangle$ form a spin singlet state with lower energy. In the presence of magnetic field, however, the Zeeman energy may overwhelm the singlet binding energy, and $|1\uparrow 2\uparrow\rangle$ or $|1\downarrow 2\downarrow\rangle$ becomes energetically favorable. Thus, CQD may have either a magnetic or a non-magnetic ground state, depending on the external magnetic field. The remaining problem is how to detect these states of CQD. We propose that by attaching CQD to two superconductors (S), spin states of CQD can be probed by measuring the dc Josephson current. The idea is illustrated in the upper part of Fig.1, and hereafter the system is referred to as S-CQD-S. It is well known that the dc Josephson current is sensitive to the spin polarization of the weak link area of the junction. For the Josephson junction coupled by an Anderson impurity (or S-QD-S heterostructure), theories show that the critical current will reverse its sign if the impurity (or QD) is singly occupied and therefore becomes a magnetic dot [14–16]. Recent experiment also reported the observation of the π-junction transition, in a Josephson junction consisting

of superconducting banks and a weakly ferromagnetic interlayer [17].

Motivated by the above facts and ideas, we will investigate the supercurrent flowing through S-CQD-S system. Different from some of the previous works, e.g. [18], we take $U \sim \Delta$ rather than $U \gg \Delta$, so that the Andreev reflection (AR) process [19,20] and the Coulomb blockade (CB) effect may "combine" with each other (U is the constant of the intra-dot Coulomb interaction, Δ is the gap of the superconducting electrodes, and the choice of $U \sim \Delta$ is physically reasonable). In the calculation, we take into account not only intra-dot but also inter-dot Coulomb interactions, both of which are found to be important in the fitting of the experimental data [4].

The suggested S-CQD-S system can be described by the following Hamiltonian,

$$H = H_L + H_{DD} + H_R + H_T \ , \tag{1}$$

in which

$$\begin{aligned} H_{DD} = \sum_\sigma E_{1\sigma} n_{1\sigma} + U_1 n_{1\uparrow} n_{1\downarrow} + \sum_\sigma E_{2\sigma} n_{2\sigma} + U_2 n_{2\uparrow} n_{2\downarrow} + \\ U_{12}(n_{1\uparrow} + n_{1\downarrow})(n_{2\uparrow} + n_{2\downarrow}) + t \sum_\sigma (c_{1\sigma}^\dagger c_{2\sigma} + c_{2\sigma}^\dagger c_{1\sigma}) \ , \end{aligned} \tag{2}$$

is for the CQD, modelled by two impurities coupled by inter-dot interaction and inter-dot tunneling ($n_{i\sigma} \equiv c_{i\sigma}^\dagger c_{i\sigma}$ is the particle number operator); H_L and H_R are standard BCS Hamiltonians for the s-wave superconducting electrodes, with superconducting phases $\phi_L = \phi/2$ and $\phi_R = -\phi/2$, respectively [21]; and H_T is tunneling Hamiltonian , connecting the three parts together.

We begin with the study of the eigen states of isolated CQD. Notice that H_{DD} can be exactly diagonalized in the particle number representation, i.e., in the set of 16 bases $|0\rangle$, $|1\uparrow\rangle, \cdots$ $|1\uparrow 1\downarrow 2\uparrow 2\downarrow\rangle$ [22]. Due to the conservation of particle number and the conservation of spin in H_{DD}, the 16×16 space can be divided into several sub-spaces,

$$16 = (1)_{\mathrm{N}=0} + (2+2)_{\mathrm{N}=1} + (1+1+4)_{\mathrm{N}=2} + (2+2)_{\mathrm{N}=3} + (1)_{\mathrm{N}=4} \ . \tag{3}$$

We have special interest in the N=2 sub-space, in which H_{DD} is expressed as

$\tilde{E}_1$					
	$\tilde{E}_2$				
		$\tilde{E}_3$	0	t	t
		0	$\tilde{E}_4$	t	t
		t	t	$\tilde{E}_5$	0
		t	t	0	$\tilde{E}_6$

(4)

with $\tilde{E}_1 = E_{1\uparrow} + E_{2\uparrow} + U_{12}$, $\tilde{E}_2 = E_{1\downarrow} + E_{2\downarrow} + U_{12}$, $\tilde{E}_3 = E_{1\uparrow} + E_{2\downarrow} + U_{12}$, $\tilde{E}_4 = E_{2\uparrow} + E_{1\downarrow} + U_{12}$, $\tilde{E}_5 = E_{1\uparrow} + E_{1\downarrow} + U_1$, and $\tilde{E}_6 = E_{2\uparrow} + E_{2\downarrow} + U_2$. For the case of identical dots [23], i.e., $U_1 = U_2 \equiv U$, $U_{12} \equiv V$, $E_{1\uparrow} = E_{2\uparrow} \equiv E_0 - h$, $E_{1\downarrow} = E_{2\downarrow} \equiv E_0 + h$, the eigen solution of H_{DD} has a simple form: $\{|1\uparrow 2\uparrow\rangle, 2E_0 - 2h + V\}$, $\{|1\downarrow 2\downarrow\rangle, 2E_0 + 2h + V\}$, $\{|\alpha_+\rangle, 2E_0 + V\}$, $\{|\beta_+\rangle, 2E_0 + U\}$, $\{|a_-\rangle, 2E_0 + V - E_b\}$, $\{|b_-\rangle, 2E_0 + U + E_b\}$, in which $|\alpha_\pm\rangle \equiv \frac{1}{\sqrt{2}}(|1\uparrow 2\downarrow\rangle \mp |1\downarrow 2\uparrow\rangle)$, $|\beta_\pm\rangle \equiv \frac{1}{\sqrt{2}}(|1\uparrow 1\downarrow\rangle \mp |2\uparrow 2\downarrow\rangle)$, $|a_-\rangle$ and $|b_-\rangle$ are the two new states perturbed from $|\alpha_-\rangle$ and $|\beta_-\rangle$. $|1\uparrow 2\uparrow\rangle$, $|1\downarrow 2\downarrow\rangle$ and $|\alpha_+\rangle$ are corresponding to the S=1 triplet states with m=1,-1,0; while $|\tilde{\alpha}_-\rangle$ is the S=0 singlet state, with a binding energy

$$E_b = \frac{1}{2}\left[\sqrt{(U-V)^2 + (4t)^2} - (U-V)\right] \quad . \tag{5}$$

With the 16 eigenstates of H_{DD}, the occupation number of CQD can be evaluated by using the relation $\langle o\rangle = Tr(\rho o)$, in which $\rho = \frac{1}{Z}e^{-\beta H}$ is the density matrix operator. The left and right insets of Fig.2 shows the occupation number per spin $\langle n_\sigma\rangle \equiv \langle n_{1\sigma}\rangle + \langle n_{2\sigma}\rangle$ vs the resonant level E_0 for different Zeeman splitting h. (In practice, E_0 can be tuned by the gate voltage, and h induced by applying an in-plane magnetic field.) The left inset is for the case of $h < h_c$, while the right is for $h > h_c$, where $2h_c \equiv E_b$ depicting the competition between the Zeeman energy and the singlet binding energy. These curves show that CQD with total electron number N=1, 3 is easily magnetized in a magnetic field, while CQD with N=2 favors a spin singlet state and only transfers to a magnetic state upon a critical magnetic field.

Next, we turn on the weak coupling between S electrodes and CQD. "Weak coupling" means that the supercurrent flowing through CQD only serves as a probe to provide the information of CQD, without disturbing the quantum states there. To include the tunneling between the two dots and the physics of AR, a 4×4 representation is introduced,

$$\mathbf{G}^{r,a,<}(\omega) \equiv \langle\langle \begin{pmatrix} c_{1\uparrow}| \\ c_{1\downarrow}^{\dagger}| \\ c_{2\uparrow}| \\ c_{2\downarrow}^{\dagger}| \end{pmatrix} \begin{pmatrix} c_{1\uparrow}^{\dagger} & c_{1\downarrow} & c_{2\uparrow}^{\dagger} & c_{2\downarrow} \end{pmatrix} \rangle\rangle_{\omega}^{r,a,<} \quad . \tag{6}$$

Notice that the retarded Green function of the isolated CQD ($\mathbf{g}^r$) can be constructed exactly by the Lehmann spectral representation,

$$\langle\langle A|B\rangle\rangle_{\omega}^{r} = \frac{1}{Z}\sum_{nm}\frac{e^{-\beta E_n}+e^{-\beta E_m}}{\omega-(E_n-E_m)+\mathrm{i}0^+}\langle m|A|n\rangle\langle n|B|m\rangle \quad , \tag{7}$$

in which n or m runs over the 16 eigenstates of H_{DD}, and A or B denotes $c_{i\sigma}$ or $c_{i\sigma}^{\dagger}$. We assume that the full Green function of S-CQD-S ($\mathbf{G}^r$) can be derived by the following approximation [24]

$$\mathbf{G}^r = \mathbf{g}^r + \mathbf{g}^r\mathbf{\Sigma}^r\mathbf{G}^r \quad , \tag{8}$$

in which $\mathbf{\Sigma}^r$ is the self-energy caused by the coupling between S electrodes and CQD. $\mathbf{\Sigma}^r$ is obtained as

$$\mathbf{\Sigma}^r = \begin{pmatrix} \mathbf{\Sigma}_L^r & 0 \\ 0 & \mathbf{\Sigma}_R^r \end{pmatrix} \quad , \tag{9}$$

in which

$$\mathbf{\Sigma}_{\beta}^r = -\frac{\mathrm{i}}{2}\Gamma_{\beta}\rho(\omega)\begin{pmatrix} 1 & -\frac{\Delta}{\omega+\mathrm{i}0^+}e^{-\mathrm{i}\phi_{\beta}} \\ -\frac{\Delta}{\omega+\mathrm{i}0^+}e^{\mathrm{i}\phi_{\beta}} & 1 \end{pmatrix} \quad (\beta = L,\ R) \ , \tag{10}$$

$$\rho(\omega) \equiv \frac{\omega+\mathrm{i}0^+}{\sqrt{(\omega+\mathrm{i}0^+)^2-\Delta^2}} \qquad (\mathrm{Im}\,\sqrt{x} > 0) \ , \tag{11}$$

and $\Gamma_{L/R}$ is the coupling strength between left / right electrode and CQD. Then the dc Josephson current flowing through S-CQD-S is obtained by the Green function technique as

$$I = \frac{2e}{\hbar}\sin\phi\int\frac{d\omega}{2\pi}f(\omega)j(\omega) \quad , \tag{12}$$

in which

$$j(\omega) = \mathrm{Im}\,J(\omega) = \mathrm{Im}\left[-\frac{\Gamma_L\Gamma_R\Delta^2}{(\omega+\mathrm{i}0^+)^2-\Delta^2}\cdot\frac{(\mathbf{g}^r)_{13}^{-1}(\mathbf{g}^r)_{24}^{-1}}{\det[(\mathbf{g}^r)^{-1}-\mathbf{\Sigma}^r]}\right] \quad , \tag{13}$$

and $f(\omega) = 1/(e^{\beta\omega}+1)$ is the Fermi distribution function. $\det[(\mathbf{g}^r)^{-1} - \mathbf{\Sigma}^r]$ in the denominator has several real roots (with infinitesimal imaginary part -i0^+) within the range of $|\omega| < \Delta$, corresponding to the Andreev bound states (ABS) in the S-CQD-S system. To avoid the divergence around these singularities, we adapt the integral path to a V-shaped contour shown in the middle inset of Fig.2 [25], as a result

$$I = \frac{2e}{\hbar}\sin\phi\,\mathrm{Im}\int_V \frac{d\omega}{2\pi} f(\omega)J(\omega) \quad . \tag{14}$$

Fig.2 shows the critical current $I_c \equiv I(\phi = \frac{\pi}{2})$ vs E_0 with different h. The curve of $h = 0$, as expected, has four CB peaks, among which are the valleys of the total electron number from N=0 to N=4. (The curve is symmetric to $E_0 = -(U/2 + 2V)$ by virtue of the electron and hole symmetry.) With the increase of h, the 1st and 4th peak are gradually suppressed [26], while the 2nd and 3rd peak exhibit a non-monotonous dependence on h: decrease first and reverse its sign to a negative peak, then increase again and diminish at sufficient large h. To understand this anomalous h dependence, we plot the curves of I_c vs h in Fig.3a, for a non-interacting S-CQD-S system by setting $U = V = 0$. (In this case, the approximate Eq.(8) becomes an exact one, and $\mathbf{g}^r$ can be evaluated explicitly.) For $h = 0$, there are two peaks in the curve separated by $2t$; for $h > 0$, I_c at $E_0 = 0$ also exhibits a non-monotonous h dependence (see the up-right inset). As we know, the supercurrent flowing through CQD is conducted mainly by the ABS, which have the property that two adjacent states carry the supercurrent with opposite signs. The spectrums of $j(\omega)$ for $h = 0, t, 2t$ are shown in the insets of Fig.3a. In each spectrum, there are four ABS denoted by $1^{\pm}$ and $2^{\pm}$ within the superconducting gap, and continuous spectrum $c^{\pm}$ outside the gap. For $h = 0$, $1^{\pm}$ and $2^{\pm}$ are distributed symmetrically to the Fermi surface $\mu = 0$. With the increase of h , these states move down toward $\omega = -\Delta$. The case of $h = t$ corresponds to three of ABS $1^{\pm}$ and 2^{-} are below the Fermi surface, while $h = 2t$ corresponds to all of them below the Fermi surface. By taking account of the Fermi distribution and the continuous spectrum contribution from $c^{\pm}$, the anomalous h dependence is readily understood. Considering the Coulomb interactions will induce more ABS in $j(\omega)$, but the h dependence of the peaks in the I_c vs E_0 curve can be explained in the similar way.

We are more interested in the supercurrent flowing in the CB valleys, since the spin states of CQD are well defined there. The curves of I_c vs h and corresponding $m \equiv \langle n_\uparrow\rangle - \langle n_\downarrow\rangle$ vs h are shown in Fig.3b, with E_0 chosen in the CB valleys of N=1, 2, 3. The two curves marked with A are typical for the supercurrent flowing in the valley with odd number, where CQD

has a net spin. Due to the strong Coulomb interaction, small magnetic field ($h \sim k_B T$) will lead to the transition of CQD from a non-magnetic molecule to a magnetic one; meanwhile, I_c reverse its sign and experiences a "π-junction" transition. The two curves marked with B, in contrast, are typical for the supercurrent flowing in the valley with even number, where CQD may choose a non-magnetic singlet or a magnetic triplet as its ground state. The transition between them occurs at the critical value of Zeeman splitting $2h_c = E_b$, with $I_c > 0$ for $h < h_c$ and $I_c \to 0^+$ for $h > h_c$. Out of our expectation, for $h \gg h_c$, $I_c \to 0^+$ instead of $I_c \to 0^-$. Roughly, this might be interpreted as the addition of two π-junction transitions, namely, the supercurrent reverse its sign after flowing through the first magnetic dot, but returns back after flowing through the second one.

To sum up, we have investigated the dc Josephson current flowing through S-CQD-S hybrid system. Our calculation is based on the exact diagonalization of coupled two impurity model and the construction of Green function in the spectral representation. To avoid the difficulty of solving the exact ABS, we choose a V-shaped integral contour in the complex ω plane. In the numerical study, we find that the dc Josephson current flowing through S-CQD-S can provide rich information of the spin polarization of CQD. The CB peaks exhibit a non-monotonous dependence on the Zeeman splitting of CQD, the current in the CB valleys can be used to probe the spin states of CQD. We believe that the proposed S-CQD-S system is within the scope of the update nano-technology in S/2DEG heterostructure, and we are looking forward to seeing the relevant experiments.

This project was supported by NSFC under Grant No. 10074001.

* To whom correspondence should be addressed.

REFERENCES

[1] F. R. Waugh *et al.*, Phys. Rev. Lett. **75,** 705 (1995).

[2] C. Livermore *et al.*, Science **274,** 1332 (1996).

[3] S. M. Maurer, S. R. Patel, and C. M. Marcus, Phys. Rev. Lett. **83,** 1043 (1999).

[4] S. D. Lee *et al.*, Phys. Rev. B **62,** R7735 (2000).

[5] C. A. Stafford and N. S. Wingreen, Phys. Rev. Lett. **76,** 1916 (1996).

[6] T. H. Oosterkamp *et al.*, Nature (London) **395,** 873 (1998).

[7] Q. -f. Sun, J. Wang, and T. -h. Lin, Phys. Rev. B **61,** 12643 (2000).

[8] M. Brodsky *et al.*, Phys. Rev. Lett. **85,** 2356 (2000).

[9] A. Georges and Y. Meir, Phys. Rev. Lett. **82,** 3508 (1999).

[10] R. Aguado and D. C. Langreth, Phys. Rev. Lett. **85,** 1946(2000).

[11] C. A. Stafford, R. Kotlyar, and S. D. Sarma, Phys. Rev. B **58,** 7091 (1998).

[12] Y. Asano, Phys. Rev. B **58,** 1414 (1998).

[13] P. Recher, E. V. Sukhorukov, and D. Loss, Phys. Rev. Lett. **85,** 1962 (2000).

[14] L. I. Glazman and K. A. Matveev, JETP Lett. **49,** 659 (1989).

[15] B. I. Spivak and S. A. Kivelson, Phys. Rev. B **43,** 3740 (1991).

[16] S. Ishizaka, J. sone, and T. Ando, Phys. Rev. B **52,** 8358 (1995).

[17] V. V. Ryazanov *et al.*, Phys. Rev. Lett. **86,** 2427 (2001).

[18] M. -S. Choi, C. Bruder, and D. Loss, Phys. Rev. B **62,** 13569 (2000).

[19] A. F. Andreev, Zh. Eksp. Teor. Fiz. **46,** 1823 (1964) [Sov. Phys. JETP **19,** 1228 (1964)].

[20] G. E. Blonder, M. Tinkham, and T. M. Klapwijk, Phys. Rev. B **25,** 4515 (1982).

[21] The chemical potentials of both superconducting electrodes are set as zero, i.e., $\mu_L = \mu_R = 0$.

[22] G. Chen, G. Klimeck, and S. Datta, Phys. Rev. B **50,** 8035 (1994).

[23] In all the numerical study, we assume that the two dots are identical, although our formula is applicable to general cases.

[24] The approximation is expected to be equivalent to a proper truncation of equation of motion, which has been tested in N-CQD-N, see C. Niu, L. -J. Liu, and T. -H. Lin, Phys. Rev. B **51,** 5130 (1995).

[25] Notice that all of the singularities of $J(\omega)$ lie in the lower half-plane.

[26] Since N=0 and N=4 correspond to empty and fully occupied CQD, they are not typical for a CB valley, and hence the 1st and 4th peak in Fig.2 are not typical for a CB peak.

FIGURE CAPTIONS

Fig. 1 Upper part: Schematic diagram of the proposed S-CQD-S system. Lower part: The four spin configurations of CQD with the total electron number N=2. (a) and (b) are for $|1\uparrow 2\uparrow\rangle$ and $|1\downarrow 2\downarrow\rangle$, respectively; (c) illustrates that $|1\uparrow 2\downarrow\rangle$ and $|1\downarrow 2\uparrow\rangle$ are coupled via high energy virtual states and forms a spin singlet.

Fig. 2 The critical current $I_c \equiv I(\frac{\pi}{2})$ vs the resonant level E_0 with different Zeeman splitting h, in units of $e = \hbar = \Delta = 1$. The parameters of CQD are: $U = 0.6$, $V = 0.2$, $t = 0.1$, due to which $h_c \approx 0.04$. The temperature and coupling strength are chosen as $k_B T = 0.01 \gg \Gamma = 0.001$, as required by the weak coupling limit. The solid, dashed, dotted, and dash-dotted curves correspond to $h = 0.00,\ 0.02,\ 0.06,\ 0.10$, respectively. The left and right insets show the occupation number per spin $\langle n_\sigma\rangle$ vs E_0 for $h = 0.02$ and $h = 0.06$, respectively. The middle inset schematically shows the singularities of $J(\omega)$ and $f(\omega)$ and the V-shaped integral contour.

Fig. 3 (a) I_c vs E_0 curves with different h, for the case of non-interacting S-CQD-S in which $U = V = 0$. The solid, dashed, dotted, and dash-dotted curves correspond to $h = 0.00,\ 0.05,\ 0.10,\ 0.20$, respectively. Other parameters are the same as those of Fig.2. The up-right inset shows I_c vs h at $E_0 = 0$, which exhibits a non-monotonous dependence. The other three insets show the spectra of $j(\omega)$ at $E_0 = 0$, with different h marked in the plots. (b) I_c vs h (solid) and corresponding $m \equiv \langle n_\uparrow\rangle - \langle n_\downarrow\rangle$ vs h (dotted), in the Coulomb blockade valleys of N=1, 2, 3. The two curves marked with A are for $E_0 = -0.95$ (also $E_0 = -0.05$), typical for CQD with odd number of electrons; the other two marked with B are for $E_0 = -0.50$, typical for CQD with even number of electrons.

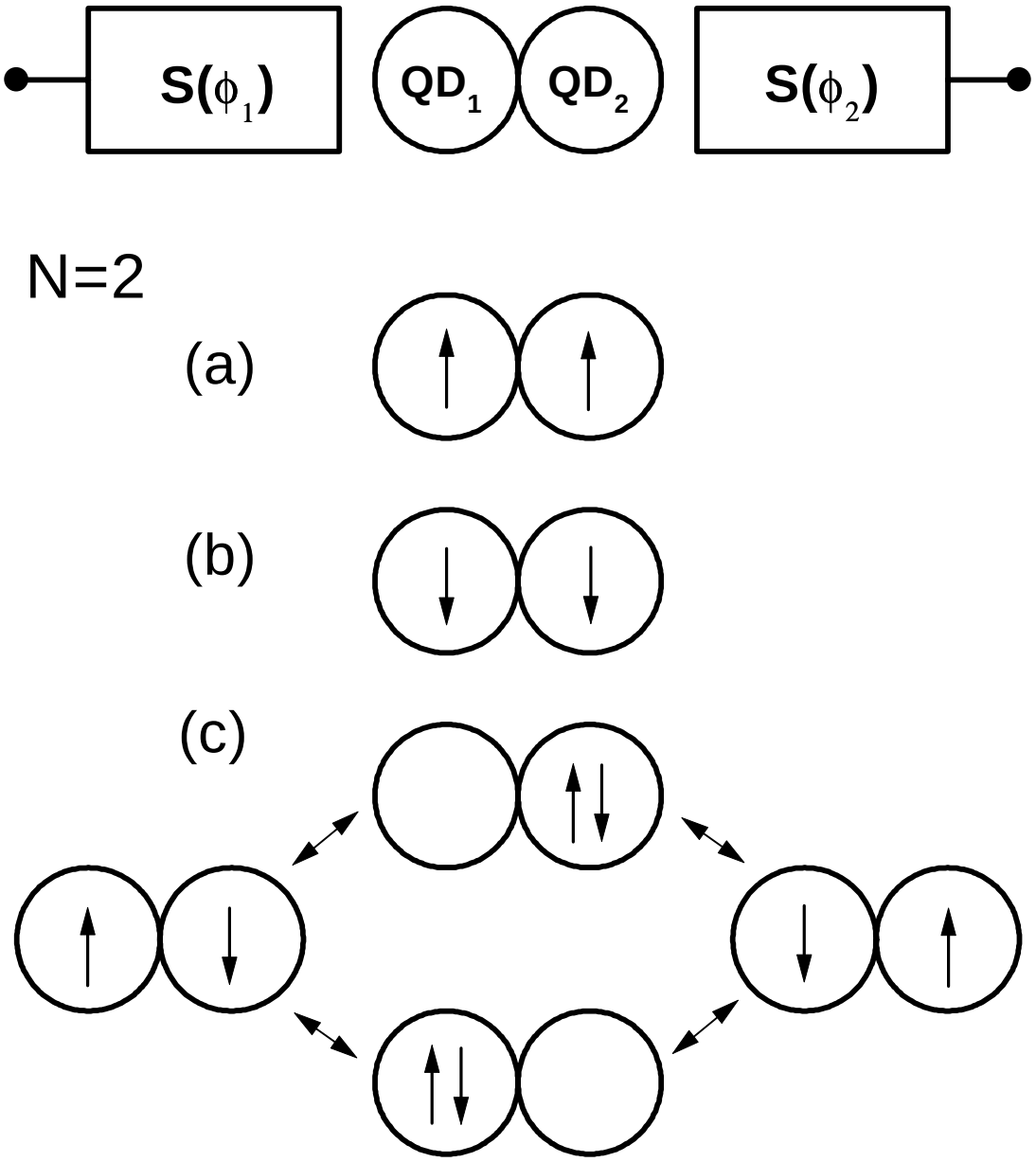

Fig.1

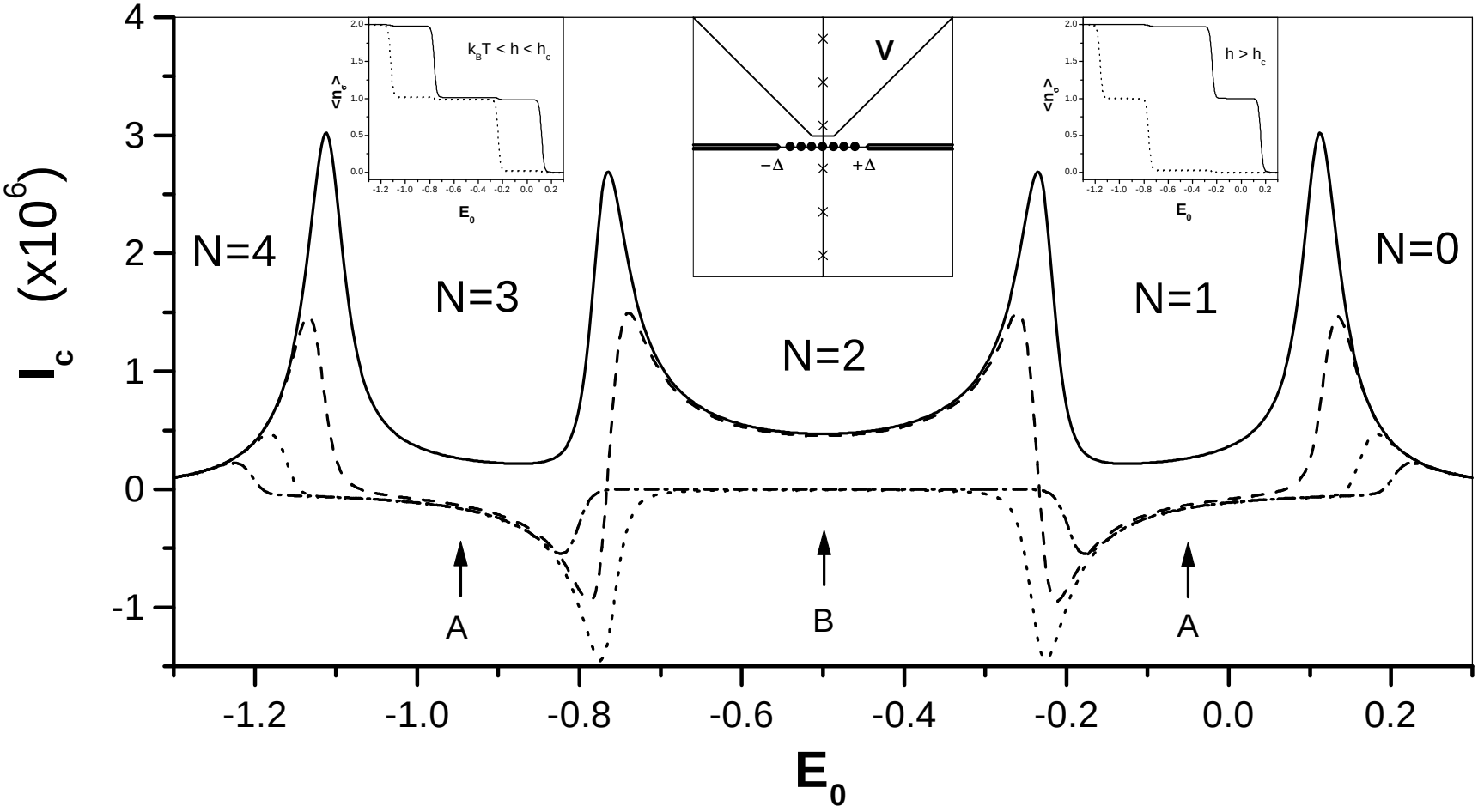
I_c (x10^6)
4
3
2
1
0
-1
N=4
N=3
N=2
N=1
N=0
A
B
A
-1.2
-1.0
-0.8
-0.6
-0.4
-0.2
0.0
0.2
E_0
$k_BT < h < h_c$
$h > h_c$
$<n_e>$
V
$-\Delta$
$+\Delta$

Fig.2

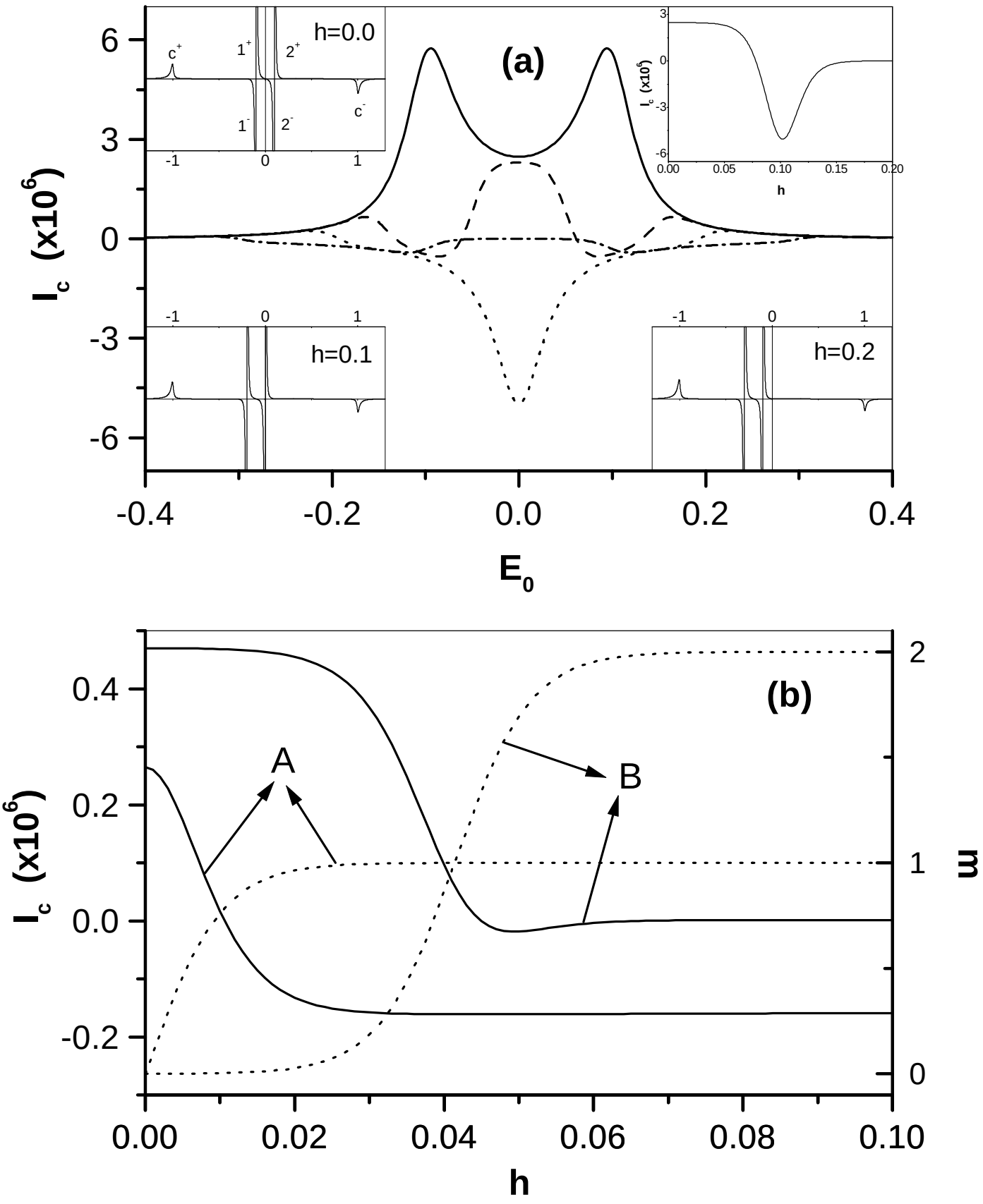

Fig.3